Proceedings of the 2nd Marine Energy Technology Symposium
METS2014
April 15-18, 2014, Seattle, WA

TIDAL DISTORTION AS PERTAINS TO HYDROKINETIC TURBINE SELECTION AND RESOURCE ASSESSMENT

Brittany Bruder *
Georgia Institute of Technology
Atlanta, GA, USA

Kevin Haas
Georgia Institute of Technology
Atlanta, GA, USA

ABSTRACT

Synthetic M_2 and M_4 velocity signals with differing relative phase, are quantified by the statistical parameters skewness and asymmetry, to observe the effect of tidal distortion on available and technical energy for hydrokinetic tidal power operations. Signals with high magnitudes of skewness have a bimodal velocity probability distribution. Asymmetric and non-distorted signals with zero skewness have singular peak values. For velocities time series with the same signal energy, such discrepancies does little to change the available kinetic energy. However, upon the application of turbine efficiency curves, technical energy output between signals with varying skewness varies up to 15%. Such discrepancies in energy outputs highlights the importance of phase, tidal distortion, and skewness for technical resource assessments

INTRODUCTION

As tides propagate through shallow waters, non-linear mechanisms grow in significance and distort the tidal signal from sinusoidal form. As a result, the tidal cycle loses symmetry; ebb and flood stages differ in duration and strength and the cycle is commonly labeled as an ebb-dominated or flood-dominated system. Such characterizations, pervasive along the US Coast, can lead to amplifications of tidal current velocities for a given stage, increasing interest in hydrokinetic energy utilization for the heavily populated coastlines. However, current enhancement in a given tidal stage implies weaker currents in the opposite stage. Hydrokinetic turbines have limited windows of operation defined by the minimum cut-in speed and maximum rated speeds and have different turbine efficiency curves as a function of velocity.

Implications of constituent phasing for power production have been previously studied by [1] and [2]. Spatial variations of constituent phasing were analyzed to identify optimum turbine installation locations and reduce intermittency in total power production for both regional [1] and national [2] scales. However, both studies concentrated on areas with relatively deep channels, small overtide amplitudes, and little distortion. The effect of the phasing between constituents and distortion of the velocity signal itself as pertains to power production was not detailed.

To further hydrokinetic energy extraction in shallow environments, the presented study analyzes the sensitivity of turbine selection and operation as a function of non-linear current velocity distributions quantified by the statistical parameters of skewness and asymmetry. First, the study presents a method to quantify tidal distortion of a velocity signal independent of the contributing constituents, the statistical parameters skewness and asymmetry. Then, synthetic velocity signals are constructed with varying values of tidal distortion. Distribution functions of velocities, available power, and energy density contribution are calculated and presented for each. Turbine efficiency curves are then implemented to observe the effect of the varying velocity distributions on technical energy density.

TIDAL DISTORTION

Tidal distortion arises from the cascade of energy from the principle astronomical tidal constituents to higher and compound harmonics known as overtides. Typically, the distortion of an estuarine system is characterized by the relative amplitude and phase of a principle constituent and its first harmonic [3]. For much of the global coasts, including the US east coast, this is the M_2 constituent and M_4 overtide, however such analysis and characterization has utilized higher harmonics as well [4]. For velocity timeseries, a larger M_4/M_2 ratio signifies a more distorted tide. The relative phasing, $\phi = 2M_2 - M_4$, indicates a longer

*Corresponding Author: bbruder1987@gatech.edu

ebb-to-flood transition ($90^\circ \pm 90^\circ$) or longer flood-to-ebb transition ($270^\circ \pm 90^\circ$), or indicates a longer flood tide ($180^\circ \pm 90^\circ$) or ebb tide ($0^\circ \pm 90^\circ$).

Although calculated constituents are an accurate characterization of tidal distortion and useful tool for model/measurement validation, they provide incomplete insight into the physical causes of the distortion. Most notably, this method can only compare two constituents at a time, disregarding other non-tidal forcing and overtide constituents. Thus, this study quantifies distortion through calculating the statistical asymmetry and skewness of the signals. Previously used for applications such as nearshore wave analysis, skewness, S_x, and asymmetry, A_x, of a signal x, are given by [5] as

$$S_x = \frac{\frac{1}{T}\sum_{t=1}^{T}(x(t)-\bar{x})^3}{(\frac{1}{T}\sum_{t=1}^{T}(x(t)-\bar{x})^2)^{\frac{3}{2}}} \tag{1}$$

and

$$A_x = S_{imag(H(x))} \tag{2}$$

respectively where T is the total number of time indices, $x(t)$ is the quantity at time index t, $\bar{x}$ is the mean of $x(t)$, and $H(x)$ represents the Hilbert Transform of x. Essentially, the asymmetry A_x, is the skewness calculation of the imaginary portion of the Hilbert transform of x.

Asymmetry, A_x, refers to the degree of symmetry about the vertical axis. For a timeseries of surface heights or fluxes, this represents the relative duration of periods of increase and decrease. For positive values of A_x, the rising period is longer than the falling, i.e. troughs appear soon after crests, but crests appear relatively later after troughs. For negative values of A_x, the falling period is longer than the rising, crests appear soon after troughs and troughs appear long after crests.

Skewness, S_x, refers to the degree of asymmetry about the horizontal axis, taking into account the relative broadness and magnitudes of the peaks and troughs. For surface height and velocity timeseries, this represents the relative duration and magnitude of high/low tide and ebb/flood durations respectively. For positive S_x, the crests have larger magnitude than the troughs and are narrower (less temporal duration above the mean) while for negative values, the troughs have larger magnitudes and are narrower.

Both A_x and S_x, when used to describe tidal signal distortion from a principle constituent and dominant overtide such as M_2 and M_4, can be related back to the relative phasing. Theoretically, velocity signals with a positive A have a longer flood-to-ebb transition and corresponds to a $2M_2 - M_4$ phase difference of $90^\circ \pm 90^\circ$ with more positive values being closer to 90° as shown in Figure 1. Positive S corresponds to a longer ebb tide and a phase difference of $(180^\circ \pm 90^\circ)$ with larger skewness values will be closer to 180° and so on. The relationship between ϕ, asymmetry, and skewness is fully shown in Figure 1.

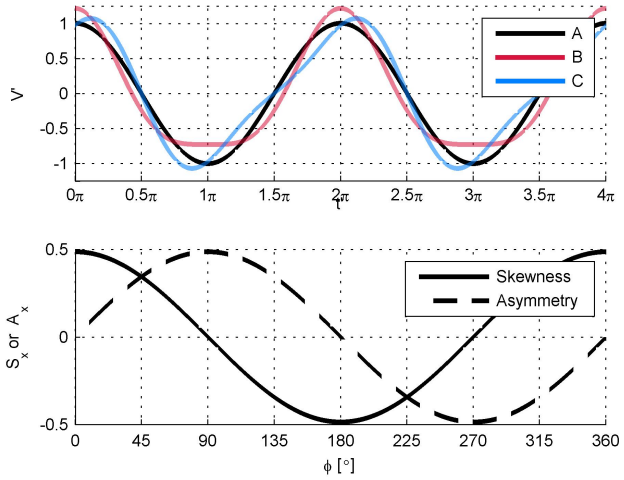

FIGURE 1. *TOP*: NON-DIMENSIONAL VELOCITY SIGNALS A ($A = S = 0$), B ($A = 0/S = 0.48/\phi = 0^\circ$), AND C ($A = 0.48/S = 0/\phi = 90^\circ$). *BOTTOM*: $M_2 + M_4$ SIGNAL SKEWNESS (SOLID) AND ASYMMETRY (DASHED) FOR VARYING ϕ.

SIGNAL CREATION + NORMALIZATION

The effects of skewness and asymmetry on tidal energy are studied through the use of two synthetic velocity signals of the form

$$V(t) = A_{M_2} cos(\omega_{M_2} t) + A_{M_4} cos(\omega_{M_4} t - \phi) \tag{3}$$

where t is time, A and ω are respectively the amplitudes and frequencies of the M_2 and M_4 constituents, and ϕ is the relative phasing of the two constituent signal contributions.

To accurately compare the aggregate effects of distortion to non-distortion, signal A is created as

$$V_A(t) = A_{M_2}\sqrt{1+r^2} cos(\omega_{M_2} t) \tag{4}$$

Signal A represents a non-distorted M_2 signal with the same *spectral* energy as a distorted signal. The amplitude of signal A is used to produce the non-dimensional velocity magnitude

$$V'(t') = \frac{|cos(t') + r cos(2t' - \phi)|}{\sqrt{1+r^2}} \tag{5}$$

where $t' = \omega_{M_2} t$ is the non-dimensional form of time. Signal B with $\phi = 0^\circ$, as shown in Figure 1, corresponds to maximum skewness and zero asymmetry while Signal C with $\phi = 90$ has zero skewness and maximum asymmetry. Both signals, have an A_{M_4}/A_{M_2} amplitude ratio, $r = 0.25$, a possible, albeit large ratio that has been observed in highly non-linear estuaries [6].

Time series of the non-dimensional kinetic power density, $P'(t')$, are created from the velocity signals as

$$P'(t') = V'(t')^3 \tag{6}$$

P' represents a fraction of the kinetic power density for the undistorted signal.

For a time varying kinetic power density such as in signals A,B and C, P' can be integrated over a period of time to provide the kinetic energy density E' defined as

$$E' = \frac{3}{8}\int_0^{2\pi} P'(t')dt' \tag{7}$$

such that E' of the undistorted Signal A is 1.0.

POWER PROBABILITY DISTRIBUTIONS

Development of Distributions

A probability density function (PDF) of V' or P' over a given tidal cycle is calculated numerically from each signal as $f_{V'}(V')$ and $f_{P'}(P')$ respectively. The mean power over the tidal cycle is then calculated as

$$\bar{P'} = \int_0^{P'_{max}} P' f_{P'} dP' \tag{8}$$

The integrand $P' f_{P'}$ can be thought of as the relative contribution to the average power output or energy for each value of P' or its respective V'.

The non-dimensional total kinetic energy density can be found as

$$E' = \frac{3}{8} 2\pi \bar{P'} \tag{9}$$

where once again the total kinetic energy density of Signal A is 1.0. Exceedence energy as a function of the cut-in power P'_c can be calculated as

$$E'_e(P'_c) = \frac{3}{8} 2\pi \int_{P'_c}^{P'_{max}} P' f_{P'} dP' \tag{10}$$

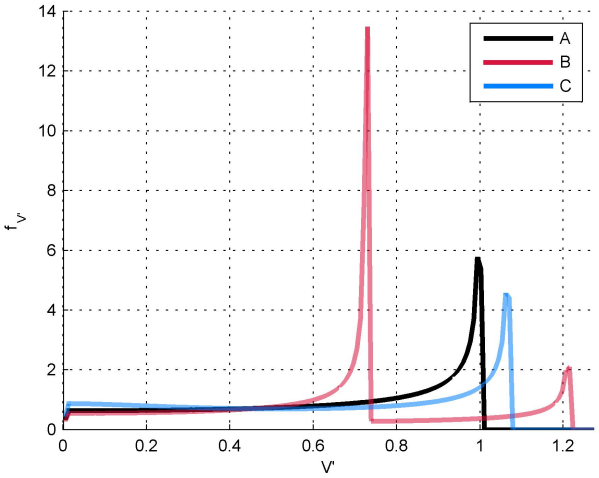

FIGURE 2. PROBABILITY DENSITY FUNCTION, $f_{V'}$ FOR NON-DIMENSIONAL VELOCITY, V', FOR SIGNALS A, B AND C

The exceedance energy $E'_e(P'_c)$ represents the total kinetic energy density in the signal produced by kinetic power densities above the cut-in power, i.e. technical kinetic energy density without the considerations of turbine efficiencies. A value of E'_e equal to one represents the full technical kinetic energy density computed from the full range of the undistorted Signal A.

As compared to a pure velocity and power PDF, plots of $f_{P'}P'$ and E'_e, help compare not only the relative distribution of powers and velocities, but also their relative *contribution* to the total energy taking into account both duration and magnitude. This assists in comparing important velocity operating ranges between signals.

Distribution Results

PDFs of velocity magnitude V' are plotted in Figure 2 for Signals A, B and C which have zero distortion, pure skewness, and pure asymmetry respectively. For all the signals, there are peaks at the corresponding velocity crest and trough magnitudes because these areas are broader than the transitional velocities at the zero-crossing. Because the trough and crest are symmetric about the x-axis for both A and C, there is only one peak in the PDF. However the higher harmonic in Signal C increases both crest and trough, resulting in a peak in the PDF with a slightly larger magnitude despite being symmetric about the x-axis.

Most striking are the double peaks for Signal B, which have maximum skewness. The first peak at a lower velocity corresponds to the weaker but broader trough velocity. Therefore the peak corresponding to the trough velocity signal is weaker at approximately 0.7 the magnitude of the undistorted signal, however has the highest peak in the PDF. Similarly, the crest magnitude, corresponds to a velocity approximately 1.2 the magnitude of the

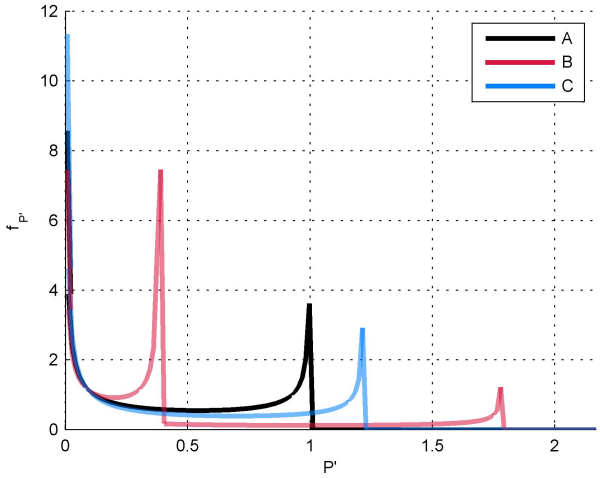

FIGURE 3. PROBABILITY DENSITY FUNCTION, $f_{P'}$ FOR NON-DIMENSIONAL KINETIC POWER DENSITY, P', FOR SIGNALS A, B AND C

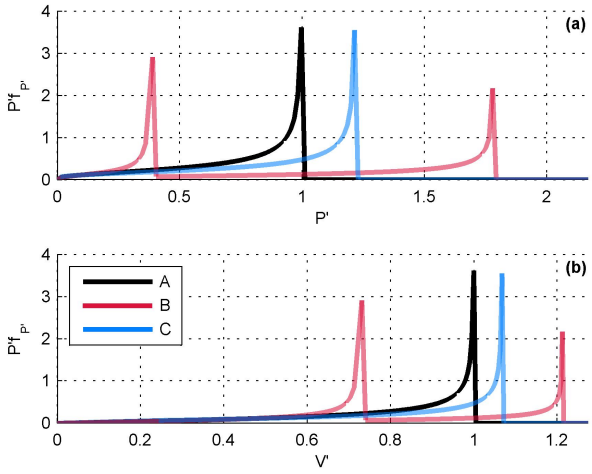

FIGURE 4. NON-DIMENSIONAL ENERGY DISTRIBUTION, $P'f_{P'}$ AS A FUNCTION OF P' *(a)* AND V' *(b)* FOR SIGNALS A, B AND C.

undistorted signal and is much narrower, therefore has a smaller peak in the PDF.

Figure 2 highlights important considerations for turbine operation and selection for distorted tides. Signals A and C have fairly large single PDF peaks for their maximum velocities whereas Signal B has the smallest pdf peak for its maximum velocity. Such discrepancies in distributions for signals with the same signal energy and relative constituent amplitudes highlights the importance of accurate phase information in resource assessments. Signal B highlights a key consideration of turbine operation and selection for skewed tides: weighing the relative contribution of the lower velocities occurring over a longer time period or the stronger currents occurring for shorter periods. To further assess this, power density distributions and energy density plots are constructed.

Figure 3 depicts a PDF for the nondimensional power density P'. Through the cube of the velocity, weak velocity signals near transitional periods are aggregated producing a large peak in the PDF near zero. This further emphasizes the additional power arisen from the increase in velocity of the distorted tides; while Signal B had 1.2 times the peak velocity of A, its peak power is now more than 1.6 that of A. Although informative on power magnitudes, Figure 3 still does not tell much about the relative contribution to energy. Although there is great representation at low P', because the actual value of $'P'$ is so small, its relative contribution to the energy is negligible. Thus inferring energy production from Figure 3 can be misleading.

As Equation 8 indicates, the mean power is formed from the integral of $P'f_{P'}$. Therefore the area under plots of $P'f_{P'}$ is an indicator of the relative contribution for each P' to the mean power and hence energy as seen from Equation 9. As seen in Figure 4(a), the large peaks at minimal velocities are diminished due to the weighing of the respective P' value as compared to the PDF in Figure 3. As expected, most of the energy is contributed by the peak velocities since peaks in the PDF corresponded to maximum power magnitudes for Signals A and C. The weighing factor of P' also reduces the difference in proportional peaks between the trough and crest magnitudes. However, Figure 4 still shows that it is the smaller trough magnitude that provides the largest energy due to its extended duration.

To facilitate assessing the implications of cut-in velocities, plots of $P'f_{P'}$ and Equation 10 are mapped back from P' to its respective V' in Figure 4b. Thus, if one were to apply a turbine with a velocity cut-in speed above 70% of the non distorted magnitude, for Signal A, a large portion of the available energy would be negated even though it has the largest crest magnitudes of the three signals. Interestingly, this would not occur for Signals A and C, despite having similar spectral energy and overall smaller crest magnitudes. At face value, a signal with a large peak velocities would seem to fair better for turbines with higher cut in speeds. However, Figure 4 highlights that this is not the case.

This concept is further explored using the exceedance energy curves defined by Equation 10 and shown in Figure 5. The exceedance energy density is normalized by the energy density of the undistorted signal. Thus the relative difference in E'_e for all signals can be treated as a direct comparison of captured energy, not relative to their own total available energy. The exceedance energy density is relatively consistent for all signals with only a small decrease until $V'_c = 0.6$. E'_e remains relatively high above 0.95, signifying only approximately 5% of the total energy of the

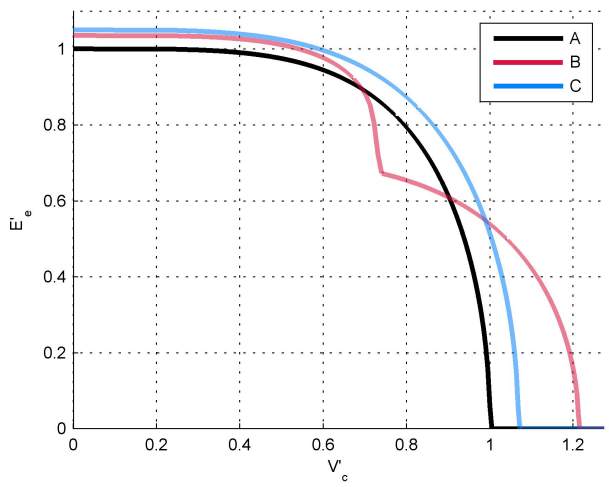

FIGURE 5. EXCEEDANCE ENERGY CURVE, E'_e FOR SIGNALS A, B AND C.

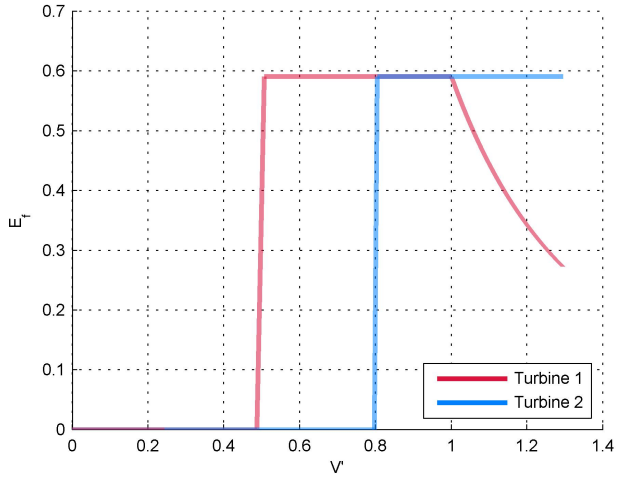

FIGURE 6. TURBINE EFFICIENCY CURVES AS A FUNCTION OF NON-DIMENSIONAL VELOCITY

undistorted signal is contained in those velocity ranges.

However, for $V'_c = 0.6 - 0.75$ there is a drastic deviation in Signal B, corresponding to the first peak seen in Figure 4. Here, E'_e drops to approximately 0.65, signifying a (0.95-.65) 30% loss of energy. Thus, it can be ascertained that the first peak for Signal B, or the trough velocities, provide approximately 30% of total energy of the signal. If a cut in speed were to be applied at $V'_c = 0.75$ with 100% uniform efficiency Signals A and C would still provide over 90% of the total available energy of the undistorted signal while Signal B, with the larger peak velocity magnitude would only provide 65%. It is not until approximately $V'_c = 0.9$ and $V'_c = 1$ where the energy captured in Signal B is greater than A and C respectively.

Although the E'_e curves clearly show the available energy incorporating cut-in speeds, it cannot highlight the effects of variable efficiencies. To accomplish this, efficiency curves are implemented and the analysis is repeated.

APPLICATION OF TURBINE EFFICIENCIES

Efficiency curves are designed as

$$E_f(V') = \begin{cases} 0 & V' \leq V'_c \\ C_D & V'_C \leq V' < V'_R \\ \frac{C_D |V'_R|^3}{|V'|^3} & V' \geq V'_R \end{cases} \tag{11}$$

where C_D is a constant efficiency or percent of the power extracted. Although arbitrary in this study since constant, it is set at 0.59 or the Betz Limit. V'_c and V'_R are the cut in and rated speeds respectively. Essentially below the cut in speed, efficiency is zero, no power is extracted. Between the V'_c and V'_R, the efficiency is constant and thus power production is consistently proportional to the increase in available energy. For velocities greater than V'_R, the turbine produces power at the rated speed, thus E_f decreases.

Two efficiency curves are constructed and plotted as a function of V' in Figure 6. Turbine 2 represents a turbine with a high cut in speed and rated speed whereas Turbine 1 represents a device with a low cut-in and rated speeds, designed for moderate currents. It is important to remember V' is not the actual cut-in speed but the ratio of the undistorted velocity magnitude; thus although a rated speed of 0.8 appears low, it can be scaled to larger values. To implement the efficiency curves into the energy production distributions, $E_f(V')$ is mapped to $E_f(P')$ and is inserted into Equation 8 providing the mean technical power

$$\bar{P}'_t = \int_0^{P'_{max}} E_f(P') P' f_{P'} dP' \tag{12}$$

The implications of the efficiency curves can be seen from the plots of $E_f P' f_{P'}$ in Figure 7. Turbine 1, designed to capture the middle of the velocity distribution, captures the large peak at moderate velocities for the skewed Signal B, but has relatively low energy production at the higher velocities compared to the available energy. The technical energy density for A, B, and C, is shown in Table 1 as 0.58, 0.49, and 0.57 respectively. Turbine 2, designed to capture the upper reaches of the velocity distribution, has technical energy densities for A, B, and C of 0.47, 0.39, and 0.51 respectively.

For Signals A and C, with singular peaks above the rated speed in Turbine 1 still has a decrease in technical energy for Turbine 2. However Signal B, which has large power production

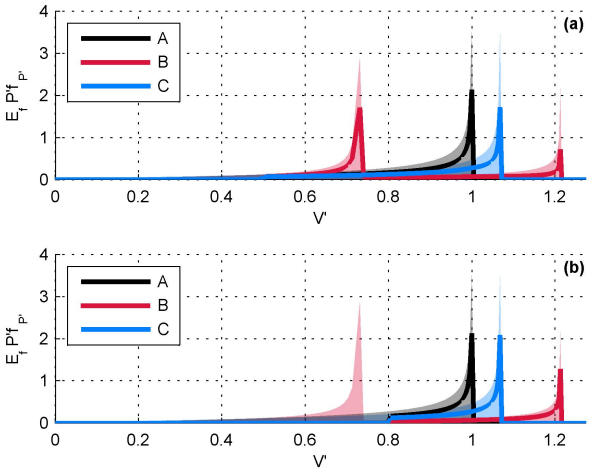

FIGURE 7. NON-DIMENSIONAL ENERGY DISTRIBUTION, $P'f_{P'}$ WITH (THICK LINES) AND WITHOUT (SHADED AREA) TURBINE EFFICIENCIES. *(a)*: TURBINE 1. *(b)*: TURBINE 2

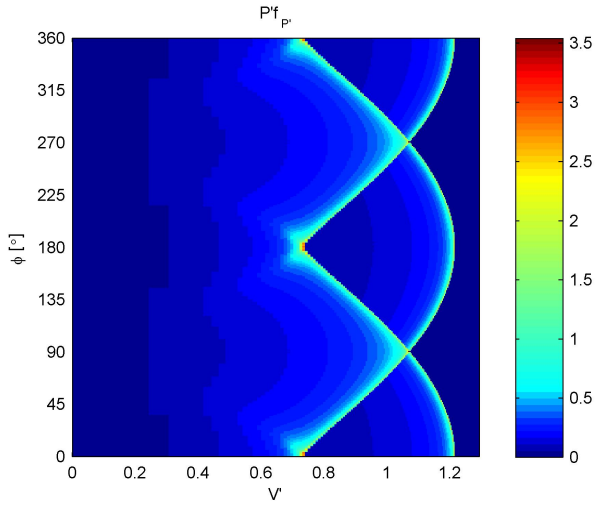

FIGURE 8. NON-DIMENSIONAL ENERGY DISTRIBUTION, $P'f_{V'}$ FOR VARYING ϕ

potential in the moderate reaches of the distribution, captures much less energy when focusing efficiency on the high velocities. Taken collectively, this is somewhat counter intuitive when tidal resource assessments are focused on peak velocity magnitudes: turbines with higher rated and cut-in speeds may not perform best for sites with large peak velocities. It also signifies the importance of accurate assessment of phase; differing values of skewness and asymmetry for for M_2/M_4 signals provided different technical resource assessments with variations up to 15% when considering the given turbine configurations.

VARYING PHASE

The comparisons of Signals B and C demonstrate the extremes of asymmetry and skewness, signals separated by 90° phase difference. It was clear in the previous analysis each signal produced clearly different velocity distributions and technical power density, particularly if certain turbine cut in speeds are applied. Thus, it is important to accurately predict the phasing and thus asymmetry and skewness of the velocity signals. However, it is anticipated most phase errors will not be on the order of 90° and the signals themselves a combination of asymmetry and skewness. Thus it is useful to analyze the power distributions for the full range of phases and asymmetry/skewness combinations to show the sensitivity of the velocity distributions to such distortion parameters.

Available Energy

Figure 8 displays the relative energy contribution of the velocities for varying ϕ. The contour plot of Signal B and C can be seen at $\phi = 0°$ and $\phi = 90°$. Signals of opposite skewness and asymmetry, negative values, can be seen at $\phi = 180°$ and $\phi = 270°$. However, because power density is a function of the absolute value of the velocity, thus disregarding sign conventions of ebb and flood, the values are the same as those at $\phi = 0°$ and $\phi = 90°$.

As ϕ ranges from maximum skewness to maximum asymmetry, the two peaks seen in Signal B appear to converge into a singular peak as seen in Signal C. Thus signals with combined asymmetry and skewness still have the concern of a bi-modal distribution, however as Skewness decreases, such peaks collapse together into one.

This is further highlighted in the exceedance energy curve seen in Figure 9. At maximum skewness ($\phi = 0°, 180°, 360°$) there is a sharp gradient in energy at approximately $V_c' = 0.7$. The decrease in energy with V_c' becomes more gradual with decreasing values of skewness. From Figure 9 it is clear that signals with increasing skewness are more susceptible to decreases in energy density from different turbine cut-in speeds.

Technical Power

The contour analysis is repeated for $E_f P' f_{P'}$ curves for both turbines and is shown in Figures 10 and 11. For Turbine 1, it is clear that the low cut in speed does little to energy production below that velocity. There is very little change between those areas in Figures 10 and 8. Visibly, only a small portion of available energy is neglected between V'=0.35m/s and 0.5 m/s. Being on the low end of the $P' f_{P'}$ distribution , this represents a small degree of energy.

However, there is significant change in the distribution of energy for the higher velocities above the rated speed $V' = 1$.

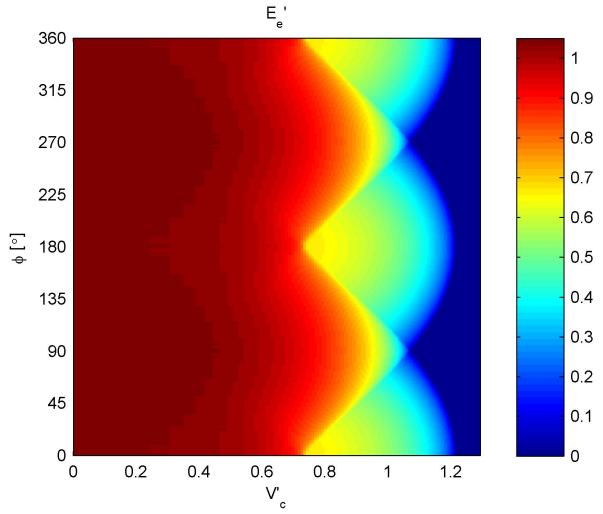

FIGURE 9. EXCEEDANCE ENERGY CURVE, E'_e FOR SIGNALS WITH VARYING ϕ

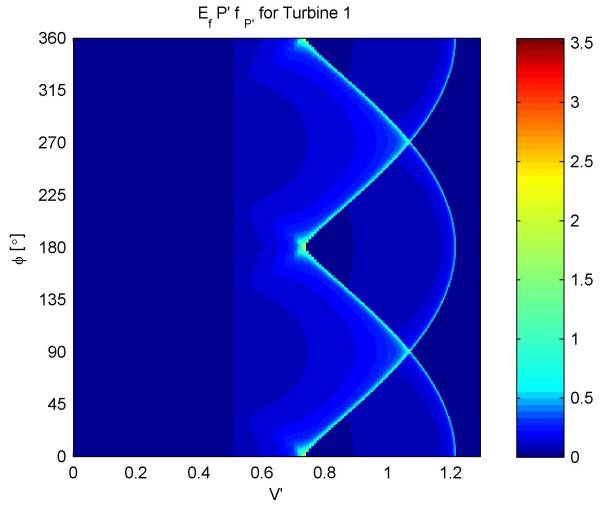

FIGURE 10. NON-DIMENSIONAL ENERGY DISTRIBUTION, $E_f P' f_{V'}$ FOR VARYING ϕ APPLYING TURBINE 1 EFFICIENCIES

In Figure 10 the breadth of the peaks is much narrower than for the available energy in Figure 8. This effect is amplified as V' increases and is a result of the rated speed capping the technical power density. Thus from Figure 10, it is clear that technical power density from high velocity signals is reduced further. As skewness grows from 0, the singular distribution of energy splits, with a small portion migrating towards higher velocities with lower efficiencies. As skewness grows, and the peak migrates towards higher velocities, efficiencies continue to drop and the energy peaks become narrower and of lesser magnitude. The larger portion of the singular peak migrates towards lower velocities with higher efficiencies and thus the breadth and intensity of these peaks remain less reduced as compared to Figure 8.

Figure 11 plots $E_f P' f_{P'}$ for Turbine 2. Here, there is little change in the distribution of energy for the larger velocities and great change in the lower as compared to Figure 8. With a relatively high cut-in speed, much of the moderate and lower velocity energy is removed. However, with a high rated speed, the distribution of energy for the higher velocities is retained. It is clear as skewness grows from 0, the distance between the splitting peaks grows. Thus, the need for a lower cut in speed, or larger operating range, grows as well.

For signals with small skewness and large asymmetry, approximately 6% less of the available energy is extracted with Turbine 2 relative to Turbine 1. However, for values with large skewness, the lower peak is clearly neglected. Thus, even though the peak at higher velocities is retained, Turbine 2 captures almost 10% less of the available energy than Turbine 1. This highlights the significance of the capturing the lower portion of the velocity distribution due to its extensive persistence in the tidal signal.

VARYING AMPLITUDE RATIO

The previous section analyzed the effect of the relative phase of the M_2 and M_4 constituent on signal skewness and asymmetry and the resultant available and technical kinetic energy density. However, the degree of distortion, the M_4/M_2 ratio r was kept fixed. In addition, with the exception of $\phi = 0°$, $90°$, $180°$, and $360°$ skewness and asymmetry were not studied in isolation with varying S and A values. Thus, to study the isolated effects of asymmetry and skewness, velocity signals are created with varying r and the non-dimensional analysis repeated. Two sets of velocity signals ARE created: one with a constant $\phi = 0°$ to observe the effect of increasing skewness alone; and one with a constant $\phi = 90°$ to observe the effect of increasing asymmetry alone.

Available Energy

For both values of ϕ, r was varied from 0 to a maximum feasible value of 0.25. It is important to note that all signals are uniquely normalized for each value of r using Equation 5. Thus, values of V' and E' refer to fraction of the undistorted value, analogous to Signal A, for each value of r. Skewness and Asymmetry were calculated for each value of r for each signal. Skewness for signals with $\phi = 0°$ and Asymmetry for signals with $\phi = 90°$, both increased with increasing r identically from a value of 0 to a maximum of 0.48.

Figures 12 and 13 show $f_{P'} P'$ and E_e plotted for signals with $\phi = 0°$. In Figure 12 it is clear that as r grows and thus the skewness, the distribution peaks split over an increasing range of velocities. In addition, the upper velocity peak becomes fainter, as the lower velocity peak becomes slightly larger in intensity. This is a result of the broadening of the trough versus the nar-

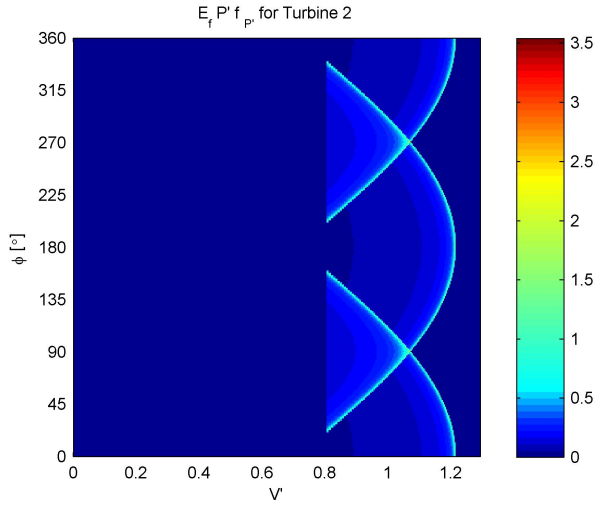

FIGURE 11. NON-DIMENSIONAL ENERGY DISTRIBUTION, $E_f P' f_{V'}$ FOR VARYING ϕ APPLYING TURBINE 2 EFFICIENCIES

TABLE 1. ENERGY PRODUCTION OF VELOCITY SIGNALS

	Signal A	Signal B	Signal C
r	0	0.25	0.25
$\phi[^\circ]$	-	0	90
Skewness	0	0.48	0
Asymmetry	0	0	0.48
E'	1	1.03	1.05
E'_T for Turbine 1	0.58	0.49	0.57
E'_T for Turbine 2	0.47	0.39	0.51

rowing of the crest. Figure 13 shows the effect of the distribution splitting on the energy exceedance curve. As in Signal A in Figure 5, there exists two distinct lobes of energy concentration. As skewness decreases, the extent of the second lobe over the velocity distribution shrinks while the first expands until collapsed into one. This signifies as skewness increases more energy is concentrated in the lower end of the velocity distribution.

Figures 14 and 15 show $f_{P'}P'$ and E_e plotted for signals with $\phi = 90^\circ$. Figure 14 highlights the expansion of the velocity distribution as Asymmetry increases; the single peak increases in velocity. Figure 15 shows the increased concentration of energy for a given V'_c as Asymmetry grows; more energy becomes concentrated near the velocity crests and troughs.

Figures 12 and 13 show similar characteristics to Figures 8 and 9 with varying M_4/M_2 phase with varying combinations of Asymmetry and Skewness. In particular, both images show the divergence of the energy distribution. Figures 12 and 14 corresponds to sections of Figures 8 and 9, from $\phi = 90^\circ$ to $\phi = 0^\circ$. However, one major difference is while the divergence in Figures 12 and 13 are relatively linear, the divergence in the corresponding sections of Figures 8 and 9 are not. This is a result of the increasing asymmetry along with the change in M_4/M_2 phase.

Figures 14 and 15 show that as Asymmetry increases, the velocity distribution extends and concentrates in slightly higher velocities. Clearly the effect of Asymmetry is much less than the effect of skewness on the available energy density. Hence the technical energy density from signals A and C are very similar.

Thus the combined effects of the Skewness and Asymmetry induced by the M_4/M_2 phasing focus energy into a singular peak for signals of high Asymmetry and focus energy into a secondary peak of lower velocity for signals with high Skewness. This reiterates again, the implications of capturing the secondary peak of lower velocity in tidal energy applications.

CONCLUSIONS

The presented study analyzes synthetic M_2 and M_4 velocity signals with differing relative phase, quantified by the statistical parameters skewness and asymmetry, to observe the effect of tidal distortion on available and technical energy for hydrokinetic tidal power operations. Large magnitudes of skewness, increases peak velocities but decreases their duration for one portion of the tidal cycle while decreases peak velocities and increases their duration for the other. Large magnitudes of Asymmetry expand the velocity distribution and redistributes more energy near peak magnitudes. Although altered in velocity magnitudes, such changes are compensated for by changes in duration; available energy of a skewed or asymmetric signal varies minimally to one of same signal energy and no distortion.

However, skewness and asymmetry alters the distribution of velocities greatly, affecting the technical energy of a signal. Depending on the turbine characteristics, it is shown technical energy assessments for a specified turbine can vary up to 15% between signals of varying skewness and asymmetry.

Applications

Conclusions from the analysis of the artificial signals can be observed in observational or modeled tidal data regardless of included constituents. Using results from a numerical Finite Volume Coastal Model (FVCOM) of Rose Dhu Island, GA, both the available and technical energy are calculated for a 43-day long time series for a given grid point [6, 7]. Current time series from two simulations with different model parameters are evaluated. The first, Simulation 1, has a skewness of -0.16, asymmetry of 0.47, and maximum current magnitude of $1.29 m/s$. Simulation 2, has a skewness of -0.34, asymmetry of 0.46, and maximum

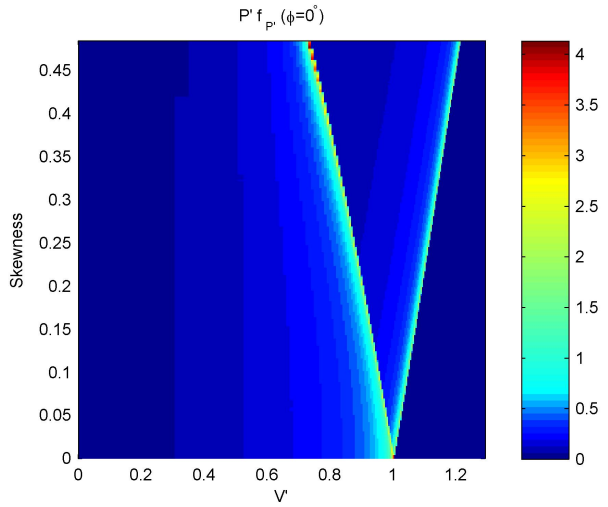

FIGURE 12. NON-DIMENSIONAL ENERGY DISTRIBUTION, $P' f_{V'}$ FOR VARYING SKEWNESS

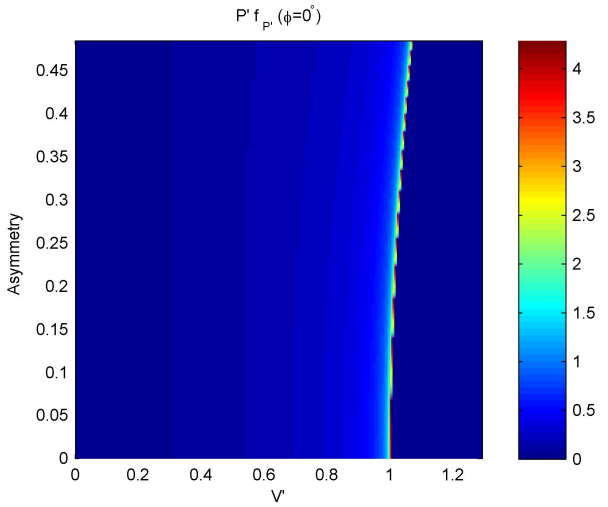

FIGURE 14. NON-DIMENSIONAL ENERGY DISTRIBUTION, $P' f_{V'}$ FOR VARYING ASYMMETRY

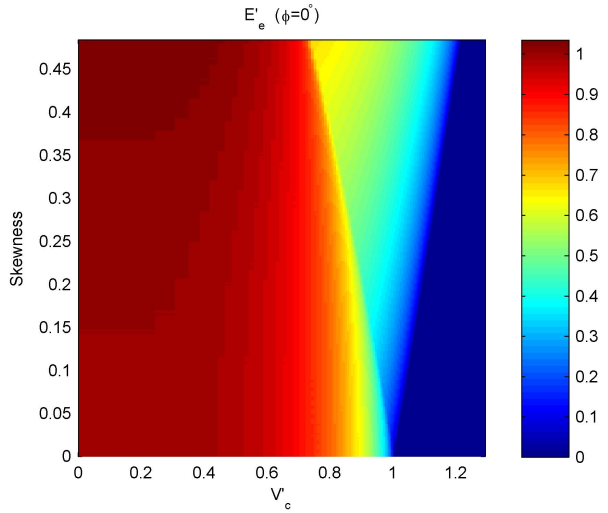

FIGURE 13. EXCEEDANCE ENERGY CURVE, $E'_e(V'_c)$ FOR SIGNALS WITH VARYING SKEWNESS

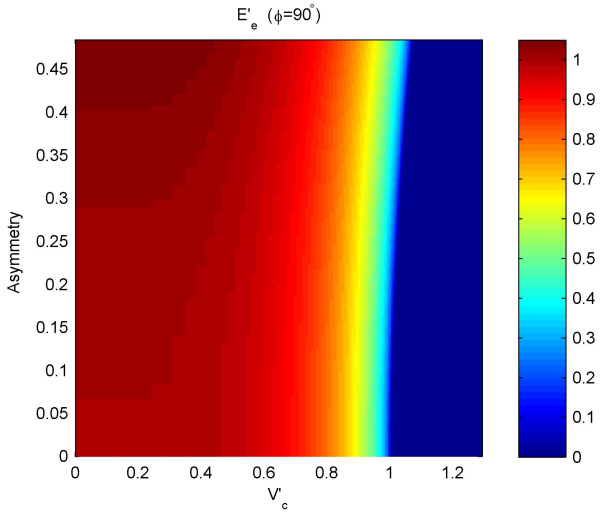

FIGURE 15. EXCEEDANCE ENERGY CURVE, $E'_e(V'_c)$ FOR SIGNALS WITH VARYING ASYMMETRY

current magnitude of $1.17 m/s$. For the technical energy assessment, cut-in and rated speeds for both turbines 1 and 2 are implemented as a fraction of the maximum current magnitude for each signal; i.e. the cut-in speed for turbine 1 for Simulation 1 was $Vc = .5(1.29) m/s$. C_D is again taken as 0.59.

Turbine 1, which captures the moderate velocities of the current range, captures 54% of the available energy of Simulation 1 and 48% for Simulation 2. Like the synthetic case, the more skewed time series provides less technical power because efficiency is lost in the higher velocities for Turbine 1. Turbine 2, which captures velocities on the higher end of the current range, captures 41% of the available energy for Simulation 1 and only 20% for Simulation 2. Again, like the synthetic time series, for highly skewed signals, technical energy is lost when the lower velocities are not captured. Despite having multiple constituents in addition to M_2 and M_4, particularly those corresponding to neap and spring tidal cycles, the analysis of the Rose Dhu model data showed similar results to that of the synthetic cases. The application of this analysis to real tidal data highlights the universality of skewness/asymmetry characterizations.

It is shown for highly skewed tidal signals, it is imperative to capture the first peak of the bimodal velocity distribution despite

having lower velocities and thus power. Because of its large duration during the tidal cycle, it provides a significant percentage of the total energy. Despite having larger peak magnitudes, the skewed signal provides more energy with turbines having lower cut-in and rated speeds in this analysis. This is in opposition to a symmetric signal, where the most efficient turbines capture the higher end of the velocity specturm with higher cut-in and rated speeds. Such discrepancies in energy outputs highlights the importance of phase, asymmetry and skewness for technical resource assessments.

ACKNOWLEDGMENT

Funding was provided by The Gray Notes Grant Program under the Ray C. Anderson Foundation. Brittany Bruder is supported by a NSF Graduate Research Fellowship under NSF GRFP Grant No. DGE-0644493.

REFERENCES

[1] Polagye, B., and Thomson, J., 2013. "Implications of tidal phasing for power generation at a tidal energy site". In Proceedings of the 1st Marine Energy Technology Symposium METS13.

[2] Iyer, A., Couch, S., Harrison, G., and Wallace, A., 2013. "Variability and phasing of tidal current energy around the united kingdom". *Renewable Energy,* ***51***, pp. 343–357.

[3] Friedrichs, C. T., and Aubrey, D. G., 1988. "Non-linear tidal distortion in shallow well-mixed estuaries: a synthesis". *Estuarine, Coastal and Shelf Science,* ***27***(5), pp. 521–545.

[4] Blanton, J. O., Lin, G., and Elston, S. A., 2002. "Tidal current asymmetry in shallow estuaries and tidal creeks". *Continental Shelf Research*.

[5] Elgar, S., and Guza, R., 1985. "Observations of bispectra of shoaling surface gravity waves". *Journal of Fluid Mechanics,* ***161***(1), pp. 425–448.

[6] Bomminayuni, S., Bruder, B., Stoesser, T., and Haas, K., 2012. "Assessment of hydrokinetic energy near rose dhu island, georgia". *Journal of Renewable and Sustainable Energy,* ***4***(6), pp. 063107–063107.

[7] Bruder, B., Bomminayuni, S., Haas, K., and Stoesser, T., 2013. "Modelling tidal distortion in the ogeechee estuary". *Ocean Modelling,* ***Submitted***.